

A Re-evaluation of the Super Li-rich Star in NGC 6633

Chris Laws

Astronomy Department, University of Washington, Seattle, WA 98195

Guillermo Gonzalez

Department of Physics and Astronomy, Iowa State University, Ames, IA 50011

ABSTRACT

We present a new abundance analysis of the super Li-rich star J37 and a comparison star in NGC 6633. We confirm the result of Deliyannis et al. that J37 has a Li abundance well above the meteoritic value, and we also confirm that Al, S, Si, Ca, Fe and Ni are super-solar, and C is sub-solar. We additionally find that Na, Sc, Ti are super-solar, while O is sub-solar. The abundance pattern of metals in J37 is generally consistent with the bulk composition of the Earth. We propose that accretion of circumstellar matter is the best explanation for these abundance anomalies, although we cannot rule out a secondary contribution from diffusion.

Subject headings: accretion - diffusion - stars:abundances - stars:atmospheres - stars:chemically peculiar - stars:evolution

1. Introduction

Deliyannis, Steinhauer, & Jeffries (2002, hereafter DSJ02) reported on their detailed abundance spectroscopic analysis of the star J37 in the open cluster NGC 6633. NGC 6633 is comparable in age to the Hyades, but it is slightly metal-poor. DSJ02 discovered that J37 has a Li abundance near $A(Li) = 4.3$ [$A(X) = 12 + \log(N_X/N_H)$], one dex above the Solar System meteoritic value. They determined abundances for eight elements, all of which were found to be enhanced above solar except C.

DSJ02 could not account for all the abundance anomalies in J37 with any known process. They favored diffusion as the best overall explanation and concluded that J37 is the first member of a previously suggested “Li peak”, covering a narrow temperature window between 6900 and 7100 K. However, they admitted that recent stellar diffusion models do not show a Li peak. DSJ02 also dismissed planetesimal accretion as a plausible explanation, owing to a poor match between the observed abundance anomalies and expectations from condensation temperature arguments – al-

though similar concerns plague the diffusion model interpretation. We will revisit both explanations in the present study.

In order to reach a better understanding of the nature of the abundance anomalies in J37, we obtained spectra of J37 and the comparison star J1 in the same cluster; DSJ02 had employed a comparison star in the open cluster M35. In the following we report on the results of our abundance analyses for both stars based on the new data.

2. Observations

Since the purpose of our study is to determine the quantitative abundance differences between J37 and its host cluster, it is necessary to select a suitable comparison star. Based on its location on the color-magnitude (CM) diagram of NGC 6633, its high probability of membership, and similar $v \sin i$, we selected J1 as the best comparison star for J37 (Jeffries et al. 2002). Unfortunately, Jeffries et al. list J1 as a probable binary based on its location on the CM diagram relative to the ZAMS. The results of our abundance analysis of J1 (presented below) yields a metallicity close to the clus-

ter mean reported by Jeffries et al., so it is unlikely that a possible companion to J1 has significantly compromised our analysis of it. We also observed J2, but subsequent analysis showed that our data were not of sufficient quality to complete a reliable analysis of this star.

We obtained optical spectra of NGC 6633 members J1, J2, and J37 over a span of approximately three hours on October 11, 2002, with the Apache Point Observatory 3.5m telescope. We employed the ARC Echelle Spectrograph and a 2048x2048 SiTe CCD, and made no changes to the instrument between the two observations. We achieved a resolving power of $\sim 37,000$ (as measured on a Th-Ar lamp spectrum) with a signal-to-noise ratio (S/N) of ~ 200 per pixel at 6700 Å. Spectra of a hot star were also obtained at a similar airmass in order to compensate for telluric features in the spectra of J1 and J37.

Data for both stars were reduced in as nearly an identical manner as possible, following the procedures described in the University of Chicago's IRAF Data Reduction Guide for the ARC Echelle Spectrograph (prepared by Julie Thompson¹). Each image was processed with the same bias and flat fields, and corrections for scattered light were made with the same fitting functions in both spectra. In addition, continua of individual orders were normalized with exactly the same functions in both stars. These steps were undertaken to minimize possible systematic differences between line depths which would ultimately impact our differential analysis. Our efforts yielded continuous one-dimensional spectra in the blue up to 4000 Å, with gaps between orders thereafter up to about 10,000 Å.

3. Analysis

The reduced spectra were examined carefully for suitable, largely unblended atomic lines. The equivalent widths (EWs) of these lines were measured following standard procedures within IRAF. Table 1 presents our adopted linelist and measured EWs for J1 and J37. Because of the relatively high stellar rotation velocities compared to cooler dwarfs, we could not employ many of the lines we have used in our previous studies of solar-type

stars. We adopted some gf -values from Gonzalez & Wallerstein (1999), and some are from accurate laboratory estimates available in the literature.

3.1. Atmospheric Parameters

We employed the measured Fe I and Fe II EWs and associated gf -values from Table 1 to derive a set of basic stellar parameters (T_{eff} , $\log g$, ξ_t , and $[\text{Fe}/\text{H}]$) and associated uncertainties for J1 and J37. All analyses utilized a recent version of the LTE abundance code MOOG (Snedden, 1973) and Kurucz model atmospheres without convective overshoot (Castelli et al. 1997²). An initial set of model atmospheres was selected with a range of values of T_{eff} , $\log g$, ξ_t , and $[\text{Fe}/\text{H}]$ centered on the results of DSJ02. Values for $\log g$ and ξ_t were then determined by systematically iterating all four of the basic parameters until the mean Fe I and Fe II abundances were equal and correlations of the individual Fe I line abundances with both χ_1 and the logarithm of reduced equivalent width (REW) were zero.

This procedure additionally yielded spectroscopic estimates of $T_{\text{eff}}(\text{spec}) = 7305 \pm 242$ for J37 and 6950 ± 223 for J1. The relatively large uncertainties in these values are due to the small number of quality Fe I lines available – especially those of low excitation potential – as well as to known non-LTE effects on Fe I abundances. The resulting uncertainty in T_{eff} is the most important source of uncertainty in subsequently derived abundances. To ameliorate this, we adopted a weighted average of our spectroscopic T_{eff} values and estimates based on photometry, using the equation presented in DSJ02 and the $B - V$ and $E(B - V)$ values quoted by Jeffries (1997). An additional possible concern is the fact that the abundance mix of J37 is significantly different from solar and that this will affect the accuracy of the photometric T_{eff} estimate.

This weighted average T_{eff} was then used with the spectroscopic $\log g$ to determine $[\text{Fe}/\text{H}]$ from linear interpolation of the MOOG Fe I and Fe II abundance results. Finally, a new set of model atmospheres were selected centered on these $T_{\text{eff}}(\text{avg})$, $\log g$, ξ_t , and $[\text{Fe}/\text{H}]$ values and the entire process iterated in metallicity until it con-

¹http://www.apo.nmsu.edu/Instruments/echelle/ARCES_data_guide.pdf

²All model atmospheres used are from <http://kurucz.harvard.edu/grids.html>.

verged.

A summary of the results of the above procedure is given in Table 2, along with estimates of absolute V-band magnitudes (M_V), theoretical values of $\log g$, and mass estimates; $[\text{Fe}/\text{H}]$ values are given in Table 1. Theoretical estimates of $\log g$, and mass are derived from our adopted $T_{\text{eff}}(\text{avg})$, M_V , and a set of 600 Myr Padova Stellar Isochrones (Jeffries et al. 2002; Salasnich et al. 2000) appropriate to each star’s metallicity.

As noted above, Fe I abundances are known to suffer from non-LTE effects. These do not affect Fe II abundances, and this difference could lead to underestimates in our spectroscopic $\log g$. We find, however, that our theoretical and spectroscopic surface gravity values are in good agreement for J1. A star of similar T_{eff} and $\log g$, HE 490 in the α Per cluster, was studied in Gonzalez & Lambert (1996) and they also found no significant offset between theoretical and spectroscopic values of $\log g$ to within their uncertainties of ~ 0.1 dex. In the case of J37, however these two differ considerably – much more so than non-LTE effects seem capable of producing. We offer a different possible explanation of this discrepancy below.

3.2. Additional Elements

Abundances for C, O, Na, Mg, Si, S, Ca, Sc, Ti, and Ni were determined in the same manner as for $[\text{Fe}/\text{H}]$, employing our measured EWs and our values of $T_{\text{eff}}(\text{avg})$ and $\log g(\text{spec})$ to interpolate the abundances from MOOG outputs. Table 1 summarizes these results, with associated uncertainties estimated from the mean deviation of line-by-line results and linear propagation of uncertainties in $T_{\text{eff}}(\text{avg})$ and $\log g(\text{spec})$. The quoted differential O abundance for J1 and J37 contains an -0.57 dex offset to account for non-LTE effects on the 7771-5 O I triplet (Takeda, 1997). The differential Na abundance has also been adjusted by -0.2 dex for non-LTE using offsets from lines of similar EWs reported in Bikmaev et al. (2002).

We determined abundances of Li and Al through comparison of the observed spectra between 6700 and 6715 Å and synthesized spectra. The latter were produced with the same set of stellar models utilized in determining $[\text{Fe}/\text{H}]$ in each star and a linelist of the region we have used in previous studies (c.f. Reddy et al. 2002). The

results are included in Table 1, with uncertainties estimated by visual inspection of synthesized spectra within an appropriate range of model conditions and elemental abundances.

Finally, we present in Table 1 $\Delta[\text{X}/\text{H}]$ values, calculated as the mean deviation of the differences in abundance values reported on a line-by-line basis between J1 and J37³. As discussed in Laws & Gonzalez (2001), such line-by-line differential comparisons eliminate systematic errors caused by uncertain gf -values and can provide a significant increase in precision over differencing the average abundances alone.

4. Discussion

4.1. Comparisons

Our abundance results for J37 are consistent with those reported by DSJ02, confirming the anomalous nature of this star. In particular, we verify that lithium is enhanced by about a factor of 10 relative to the Solar System meteoritic value. In addition, iron is about half a dex higher than the solar value, while carbon is strongly depleted. We do find a lower sulfur abundance than DSJ02, but their estimate for this element was based on only one line.

4.2. Possible causes of abundance pattern

J37 is a late A or early F dwarf, and as such, it should possess a very shallow convection zone. This relatively thin mixing layer allows certain processes to produce observable effects that are mostly negligible in cooler dwarfs. Two that have been discussed in the literature are accretion and diffusion. DSJ02 favored diffusion as the best explanation for the abundance pattern in J37. In light of the new observations we present in this study, we revisit these two hypotheses below.

4.2.1. Diffusion

Richer, Michaud, & Turcotte (2000, hereafter RMT00) present models that include the effects of atomic and turbulent diffusion transport in an effort to account for the abundance trends observed in AmFm stars. They are successful in accounting

³ $\Delta[\text{Li}/\text{H}]$ and $\Delta[\text{Al}/\text{H}]$ Li are exceptions to this, and are simply the differences between the reported abundances of the spectral syntheses)

for the general abundance patterns seen, especially the increase in abundance with atomic number. There do still exist some significant discrepancies between the models and observations, but it is not clear how much can be attributed to observational versus theoretical uncertainties.

DSJ02 argued that the diffusion model abundances of RMT00 offer the best explanation for the anomalous abundance pattern of J37 in relation to a comparison star in M35. DSJ02 note that the theoretical results of RMT00 are consistent with their abundance estimates for C, Fe, and Ni. However, they also note that their abundance estimates for S, Si, Al, Ca, and especially Li (but see below) are too high compared to the predictions of RMT00.

We added four elements not measured by DSJ02 in J37: O, Na, Sc, and Ti. While our LTE analysis of the 7771-5 O triplet showed very similar oxygen abundances for J1 and J37, the non-LTE corrections for abundances derived from these features (Takeda, 1997) yield a considerable differential offset between these two stars, resulting in J37 appearing depleted in O by 0.57 dex relative to J1. Na, Sc, and Ti, however are significantly enhanced relative to J1. RMT00 predict O to be depleted, Sc and Ti to be slightly enhanced, and Na to be slightly depleted. Our lower abundance value for S than DSJ02 mitigates the disagreement with RMT00, but it is still too high. In summary, then, the predictions of RMT00 are not in agreement with the observed abundances of the elements Li, Na, S, Si, Al, Ca, and Sc, while they are consistent with C, O, Fe, and Ni (and possibly Ti). The very low abundance of C and the non-LTE corrected O abundance are the strongest evidence for diffusion in J37. We compare in Figure 1 our abundance results to the abundances of 63 Tau and the best-fit diffusion model from RMT00; 63 Tau is an A star in the Hyades cluster with a similar T_{eff} to J37.

DSJ02 suggested the high abundance of Li could be explained by the theoretical model of Richer & Michaud (1993). However, they also noted that the more recent models of RMT00 no longer showed enhancement of Li. The Li enhancement predicted by Richer & Michaud displays a narrow peak centered just below 7100 K for $[\text{Fe}/\text{H}] = -0.15$. DSJ02 find that J37 falls on the hot side of the predicted Li-peak. Our slightly higher

T_{eff} for J37 puts it even farther from the predicted peak. At the same time, our analysis places J1 on the cool side of the predicted Li-peak, yet it displays no apparent Li enhancement.

4.2.2. Accretion

Alexander (1967) first proposed that the surface composition of a star could be measurably altered by the accretion of H-depleted material; specifically, he argued that an old star could experience dramatic enhancement of its Li abundance with the accretion of a planet like Jupiter. Brown et al. (1989) revived the idea to try to account for the very high Li abundances observed in some field red giant stars. Gonzalez (1998) suggested that planet accretion might account for unusual observed stellar atmospheric abundances – this time for Sun-like stars with giant planets.

Laws & Gonzalez (2001) and Gratton et al. (2001) present evidence for the alteration of the surface abundances of stars in wide binaries (16 Cyg and HD 219542, respectively) by accretion of H-depleted material. The components of 16 Cyg and HD 219542 (all G dwarfs) display slightly different metallicities, and even different trends with condensation temperature, a strong sign of accretion of fractionated material. The sense of the trend is such that elements with high condensation temperature have higher abundances compared to most stars. The abundances are enhanced by less than a tenth of a dex in these cases.

The interstellar medium gas phase abundances correlate strongly with condensation temperature. This is interpreted as resulting from preferential condensation onto grains by elements with high condensation temperature. Two classes of stars are observed to display abundances that correlate with the interstellar abundances: post-AGB and λ Boo stars. The former are in a highly evolved stage, while the latter are young (late B to early F dwarfs). The post-AGB class includes variables (Giridhar et al. 2000) and non-variables (van Winckel et al. 1992). For example, Giridhar et al. find that those RV Tauri variables showing evidence of depletion often have Al/Fe, Ca/Fe, and Sc/Fe ratios below solar, while C/Fe, O/Fe, S/Fe, and Na/Fe are above solar. Because populations I and II are present among the post-AGB stars, it is not always clear what the original abundances were prior to selective depletion. It is usually as-

sumed that the original abundance scale is given by their S and Zn abundances.

λ Boo stars display above-solar ratios for C/Fe, N/Fe, O/Fe, S/Fe and below-solar ratios for Ca/Fe and Ti/Fe. Venn & Lambert (1990) proposed that the abundance pattern of λ Boo stars derive from their local circumstellar or interstellar environment, given their correlation with the interstellar gas phase abundances. Heiter (2002) reviews the abundance patterns of λ Boo stars using all available data published through 2001. Interestingly, they find that Na is often enhanced above solar, and the Ni/Fe ratio is also enhanced; Andrievsky et al. (2002) confirm the high Na abundances in some λ Boo stars. Heiter et al. (2002) confirmed that the abundances of λ Boo stars do correlate with the interstellar abundances in general, but they differ in detail. Paunzen et al. (1999) have found very low C abundances for some λ Boo stars, but there is still some controversy concerning C abundances determined from near infrared versus optical lines.

Thus, at present there is observational evidence for two processes that can alter the surface abundances of stars as a result of accretion of fractionated material. In one case, material depleted in low-condensation temperature elements accretes onto a star and enhances the abundances of elements with high condensation temperature. In the other, gas selectively depleted in high condensation temperature elements via grain condensation and loss is accreted onto a star, resulting in depletion of the high condensation temperature elements in its atmosphere. In the first case, relatively small amounts of accreted material can cause observed surface abundance changes in a star, while in the second, most of the mass of a star's convective envelope must be composed of accreted gas.

4.2.3. *Diffusion and Accretion?*

Can we select one process over the other in the case of J37? Based on the above discussion, it appears that neither diffusion nor accretion (of either type) is completely consistent with its abundance pattern. Its low C and O abundances and above-solar Ni/Fe ratio are consistent with diffusion, but the high Li, Na, Mg, Al, Si, S, Ca, Sc, and Ti abundances are not consistent with it. Its overall abundance pattern does correlate with condensa-

tion temperature, but there are some anomalies, such as the high Na abundance and low C/O and high Ni/Fe ratios.

Diffusion and accretion processes are observed over the same range in spectral type: A-F dwarfs. Both processes are most effective for stars with a shallow convection zone. Therefore, it would be reasonable to expect that many stars should display the effects of both, though in most cases one or the other will dominate. Until now, studies have focused on either diffusion or accretion to explain the non-solar abundance patterns among early-type dwarfs. Perhaps we have yet to see a completely clean signature of either process operating in a given star.

J37 is near the cool end of the A and F stars observed to have abundance anomalies. Its rotation is also slower than most A and early F stars ($v \sin i = 32 \text{ km s}^{-1}$ according to DSJ02; we find 25 km s^{-1} in our syntheses). For example, most λ Boo stars studied to date have $v \sin i$ between 50 and 100 km s^{-1} . Slow rotators are expected to have less meridional circulation, which tends to dilute surface abundance anomalies. Given this, J37 might display abundance anomalies more clearly than otherwise similar stars with faster rotation.

We can combine three separate processes with various weights to account for the abundances of J37: accretion of planetesimals, accretion of gas depleted of refractories, and diffusion. Unfortunately, neither diffusion theory proposed for AmFm stars nor accretion scenarios proposed for λ Boo stars can account for all the abundance anomalies observed in A and F dwarfs. In addition to comparing the abundances of J37 to theory, we should also compare them to the observed patterns. If we take into account all the abundance anomalies noted among the λ Boo stars, we could account for its low C and high Na abundances and high Ni/Fe ratio. To further account for the high iron-peak abundances in J37, we can add either diffusion or planetesimal accretion. The most serious problem with diffusion as an explanation for J37 is its prediction of low Li, Ca, Sc, and Ti. But, Ca, Sc, and Ti are also observed to be depleted in λ Boo stars. Thus, planetesimal accretion is also needed.

The composition of accreted planetesimals is important. To account for the low C abundance in J37, they must be depleted in C. But, at the same

time, they should not be strongly depleted in Na or S. The bulk Earth fits these requirements rather well, except that Na and S are probably a bit too low in the Earth. Table 3 presents $[X/Fe]$ values for J37-J1, terrestrial material (see Gonzalez et al. 2001 for details), mean λ Boo (Heiter 2002), and both 63 Tau and a best-fit diffusion model for it (RMT00).

Either diffusion or accretion will result in an enhancement of metals in the surface layers of a star. The result of this is a spectroscopic $\log g$ value which is smaller than predicted from stellar evolutionary models which assume homogeneous composition (Laws et al. 2003). Our spectroscopic estimate of surface gravity for J37 is indeed much lower than that predicted by the Padova isochrone set (see Table 2), and likely lower than a simple non-LTE correction could account for.

In summary, we suggest that the elements in the convection zone of J37 were set by the composition of: (a) the primordial gas from the star's formation, (b) subsequent accretion of both depleted circumstellar gas and planetesimal material, and (c) evolution of its atmosphere through internal processes (diffusion, growth of the convective zone, etc.). The timing of each of these is not clear at this time, and some of these processes would certainly affect the others. For example, the accretion of planetesimals would increase the metallicity of the atmosphere, and, as a result, deepen the convection zone and reduce the efficiency of diffusion.

5. Conclusions

We have obtained and analysed high quality echelle spectra of J37 and J1 in NGC 6633. Our estimates of elemental abundances are consistent with those reported by DSJ02 for J37, and we additionally analysed four elements not measured by DSJ02: O, Na, Sc, and Ti. Overall, we find that the abundance pattern of J37 shows a very poor match to the predictions of recent diffusion models, and while we do not rule out diffusion as a factor in the abundance anomalies seen in J37, it appears to play at best a secondary role. We suggest instead that accretion of circumstellar material provides the best match. Although no single accretion source seems completely consistent with the abundance pattern of J37, we note that the accretion of material depleted in C, like that of the bulk

Earth, is implied. Precisely how much condensed material and/or depleted gas the star would need to accrete, however, and whether or not that was reasonable given the environment and evolutionary state of the star, are details that are difficult to determine at this time. A larger sample of comparison stars and detailed observations of their circumstellar environments (including that of J37) are needed to constrain environmental variables, while further developments in stellar models including accretion and diffusion processes are also necessary in order to fully resolve the abundances anomalies observed in this unusual star.

This work has been supported by the University of Washington Astrobiology Program and a grant from the National Astrobiology Institute. Additionally, this research has made use of the Simbad database, operated at CDS, Strasbourg, France.

REFERENCES

- Alexander, J. B. 1967, *Observatory*, 87, 238
- Andrievsky, S. M., Chernyshova, I. V., Paunzen, E., Weiss, W. W., Korotin, S. A. et al. 2002, *A&A*, 396, 641
- Bikmaev, I. F., Ryabchikova, H. Bruntt, Musaev, F. A., Mashonkina, L. I., Belyakova, E. V., et al. 2002, *A&A*, 389, 537
- Brown, J. A., Sneden, C., Lambert, D. L., & Dutchover, E. 1989, *ApJS*, 71, 293
- Castelli, F., Gratton, R. G., & Kurucz, R. L., 1997, *A&A*, 318, 841
- Deliyannis, C. P., Steinhauer, A., & Jeffries, R. D. 2002, *ApJ*, 577, L39
- Giridhar, S., Lambert, D. L., & Gonzalez, G. 2000, *ApJ*, 531, 521
- Gonzalez, G. 1998, *AJ*, 334, 221
- Gonzalez, G., Laws, C., Tyagi, S., & Reddy, B. E. 2001, *AJ*, 121, 432
- Gonzalez, G., & Lambert, D. 1996, *AJ*, 111, 424
- Gonzalez, G., & Wallerstein, G. 1999, *AJ*, 117, 2286

Gratton, J., Michaud, G., & Turcotte, S. 2000, ApJ, 529, 338

Heiter, U. 2002, A&A, 381, 959

Heiter, U., Weiss, W. W., & Paunzen, E. 2002, A&A, 381, 971

Jeffries, R. D. 1997, MNRAS, 292, 177

Jeffries, R. D., Totten, E. J., Harmer, S., & Deliyannis, C. P. 2002, MNRAS, 336, 1109

Kurucz, R. L. 1993, ATLAS9 Stellar Atmosphere Programs and 2km/s Grid CDROM Vol. 13, Smithsonian Astrophysical Observatory

Laws, C., & Gonzalez, G. 2001, ApJ, 553, 405

Laws, C., Gonzalez, G., Walker, K. M., Tyagi, S., Dodsworth, J., et al. 2003, ApJ, 125, 2664

Paunzen, E., Kamp, I., Iliev, I. Kh., et al. 1999, A&A, 345, 597

Reddy, B. E., Lambert, D. L., Laws, C., Gonzalez, G., & Covey, K. 2002, MNRAS, 335, 1005

Richer, J., & Michaud, G. 1993, ApJ, 416, 312

Richer, J., Michaud, G., & Turcotte, S. 2000, ApJ, 529, 338 (RMT00)

Salasnich, B., Girardi, L., Weiss, A., & Chiosi, C. 2000, A&A, 361, 1023S

Snedden, C. 1973, PhD Thesis, University of Texas

Takeda, Y. 1997, PASJ, 49, 471

van Winckel, H., Mathias, J., & Waelkens, C. 1992, Nature, 356, 500

Venn, K., & Lambert, D. L. 1990, ApJ, 363, 234

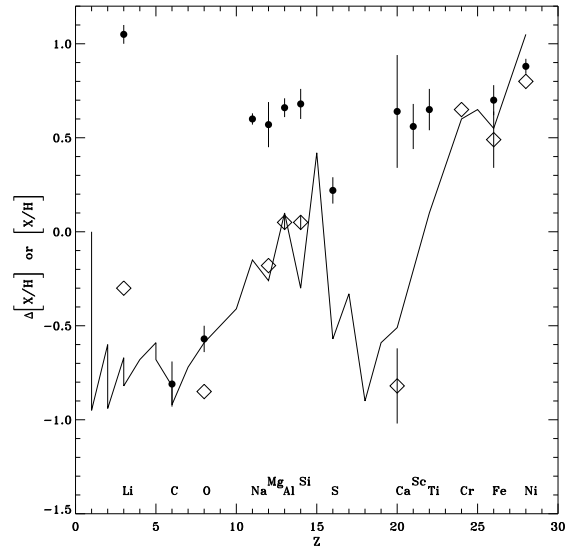


Fig. 1.— $\Delta[X/H]$ values for J1 and J37 (filled circles) from this study. Also shown are $[X/H]$ values for 63 Tau (diamonds) and a best-fit model that includes diffusion (line), both from RMT(00). Error bars are included for those elements in 63 Tau for which uncertainty estimates were provided in RMT(00).

TABLE 1
SPECTRAL RESULTS FOR J 1 AND J 37

Species	$\lambda_o(\text{\AA})$	EW_{J1}	EW_{J37}	$[X/H]_{J1}$	$[X/H]_{J37}$	$\Delta[X/H](J37 - J1)$
C I	6587.62	61.7	< 31.4			
C I	7115.18	64.4	< 37.1			
C I	8335.15	219.0	165.5			
ave C	$+0.07 \pm 0.04$	-0.74 ± 0.12	-0.81 ± 0.12
O I	7771.95	241.3	285.9			
O I	7774.18	205.1	260.0			
O I	7775.40	177.7	216.7			
ave O	$+0.63 \pm 0.07$	$+0.58 \pm 0.10$	-0.57 ± 0.07^a
Na I	8183.25	184.2	261.0			
Na I	8194.84	234.9	315.0			
ave Na	$+0.08 \pm 0.01$	$+0.87 \pm 0.04$	$+0.60 \pm 0.03^b$
Mg I	8717.83	69.9	139.3			
ave Mg	-0.04 ± 0.15	$+0.53 \pm 0.14$	$+0.57 \pm 0.12$
Si I	6145.02	17.5	57.0			
Si I	6721.85	30.8	64.8			
Si I	8556.80	138.7	235.2			
ave Si	-0.13 ± 0.16	$+0.56 \pm 0.19$	$+0.68 \pm 0.08$
S I	6046.02	31.7	68.0			
S I	6757.19	47.9	80.0			
ave S	$+0.14 \pm 0.11$	$+0.36 \pm 0.18$	$+0.22 \pm 0.07$
Ca I	5857.46	121.6	211.7			
Ca I	6439.08	180.5	221.6			
ave Ca	$+0.06 \pm 0.10$	$+0.71 \pm 0.19$	$+0.64 \pm 0.30$
Sc II	6604.60	21.1	75.2			
ave Sc	-0.27 ± 0.16	$+0.30 \pm 0.15$	$+0.56 \pm 0.12$
Ti II	5336.77	81.9	174.8			
ave Ti	-0.18 ± 0.13	$+0.47 \pm 0.15$	$+0.88 \pm 0.11$
Fe I	5434.52	136.9	204.7			
Fe I	5862.35	60.9	121.1			
Fe I	6027.06	36.9	81.9			
Fe I	6056.01	53.8	103.0			
Fe I	6065.48	88.9	149.0			
Fe I	6380.74	18.6	50.4			
Fe I	6677.99	91.6	182.4			
Fe I	6750.16	35.3	62.4			
Fe I	7507.27	32.1	78.4			
Fe I	7568.91	50.8	93.1			
Fe I	7583.80	37.5	82.6			
Fe I	7586.03	75.6	143.4			
Fe I	8327.05	129.8	175.7			
Fe I	8468.40	81.2	178.1			
Fe II	6084.17	30.9	82.5			
Fe II	6149.25	58.0	164.5			
Fe II	6369.45	117.3	...			
Fe II	6416.99	51.1	155.4			
ave Fe	-0.19 ± 0.14	$+0.51 \pm 0.16$	$+0.70 \pm 0.08$
Ni I	6643.64	33.3	93.5			
Ni I	6767.78	26.5	73.7			
ave Ni	-0.44 ± 0.08	$+0.45 \pm 0.05$	$+0.88 \pm 0.04$
Li ^b	$+2.04 \pm 0.05$	$+3.09 \pm 0.05$	$+1.05 \pm 0.05$
Al ^b	-0.14 ± 0.05	$+0.52 \pm 0.04$	$+0.66 \pm 0.05$

TABLE 2
STELLAR PARAMETERS FOR J 1 AND J 37

Star	M_V^a	$T_{\text{eff}}(\text{spec})$ (K)	$T_{\text{eff}}(\text{phot})^b$ (K)	$T_{\text{eff}}(\text{avg})$ (K)	ξ_t (km s $^{-1}$)	$\log g_{\text{spec}}$	$\log g_{\text{evol}}^c$	Mass c (M_\odot)
J 1	3.47 ± 0.20	6950 ± 223	6828 ± 103	6849 ± 93	2.39 ± 0.18	4.36 ± 0.23	4.31 ± 0.10	1.31 ± 0.05
J 37	3.15 ± 0.20	7305 ± 242	7122 ± 93	7145 ± 87	3.43 ± 0.13	3.53 ± 0.33	~ 4.28	~ 1.45

^aCalculated from an NGC 6633 distance modulus of 7.77 (Jeffries et al. 2002).

^bUsing the formula given in DSJ02 and $B - V$ colors of Jeffries (1997).

^cDerived from 600 Myr Padova Stellar Isochrones (Jeffries et al. 2002; Salasnich et al. 2000).

TABLE 3
[X/Fe]

Element	J 37 - J 1	Earth ^a	mean λ Boo ^b	63 Tau ^c	Diffusion model ^c
Li	+0.35	-0.18	...	-0.79	-1.30
C	-1.51	-4.21	+1.00	...	-1.42
O	-1.27	-0.79	+0.70	-1.34	-1.14
Na	-0.10	-0.56	+1.20	...	-0.70
Mg	-0.13	-0.05	+0.00	-0.67	-0.81
Al	-0.04	+0.00	-0.50	-0.44	-0.45
Si	-0.02	-0.09	+1.20	-0.44	-0.85
S	-0.48	-1.14	+0.70	...	-1.12
Ca	-0.06	+0.00	+0.00	-1.31	-1.06
Sc	-0.14	-0.04	-0.10
Ti	-0.05	-0.05	+0.10	...	-0.45
Ni	+0.18	-0.04	+0.30	+0.31	+0.50

^aSee Gonzalez et al. (2001).

^bFrom Heiter (2002).

^cFrom RMT00.